SMC is recruited to oriC by ParB and promotes chromosome segregation in Streptococcus pneumoniae

Minnen, Anita; Attaiech, Laetitia; Thon, Maria; Gruber, Stephan; Veening, Jan-Willem

Published in:
Molecular Microbiology

DOI:
10.1111/j.1365-2958.2011.07722.x

Publication date:
2011

Molecular Microbiology (2011) 81(3), 676–688 ■
doi:10.1111/j.1365-2958.2011.07722.x
First published online 22 June 2011

SMC is recruited to *oriC* by ParB and promotes chromosome segregation in *Streptococcus pneumoniae*

Anita Minnen,[1†] Laetitia Attaiech,[1†] Maria Thon,[1] Stephan Gruber[2] and Jan-Willem Veening[1*]**
[1]*Molecular Genetics Group, Groningen Biomolecular Sciences and Biotechnology Institute, Centre for Synthetic Biology, University of Groningen, Nijenborgh 7, 9747 AG, Groningen, The Netherlands.*
[2]*Max-Planck-Institute of Biochemistry, Am Klopferspitz 18, 82152 Martinsried, Germany.*

Summary

Segregation of replicated chromosomes is an essential process in all organisms. How bacteria, such as the oval-shaped human pathogen *Streptococcus pneumoniae*, efficiently segregate their chromosomes is poorly understood. Here we show that the pneumococcal homologue of the DNA-binding protein ParB recruits *S. pneumoniae* condensin (SMC) to centromere-like DNA sequences (*parS*) that are located near the origin of replication, in a similar fashion as was shown for the rod-shaped model bacterium *Bacillus subtilis*. In contrast to *B. subtilis*, *smc* is not essential in *S. pneumoniae*, and Δ*smc* cells do not show an increased sensitivity to gyrase inhibitors or high temperatures. However, deletion of *smc* and/or *parB* results in a mild chromosome segregation defect. Our results show that *S. pneumoniae* contains a functional chromosome segregation machine that promotes efficient chromosome segregation by recruitment of SMC via ParB. Intriguingly, the data indicate that other, as of yet unknown mechanisms, are at play to ensure proper chromosome segregation in this organism.

Introduction

The Gram-positive bacterium *Streptococcus pneumoniae* is a commensal of the human nasopharynx. Under specific circumstances however, it behaves as a pathogen and can cause diverse pathologies such as pneumonia, meningitis, otitis media and sepsis (Weiser, 2010). Over the last decades *S. pneumoniae* resistance to antimicrobial drugs has spread and is now a serious problem (O'Brien *et al*., 2009; van der Poll and Opal, 2009; Lynch and Zhanel, 2010; Mitchell and Mitchell, 2010). To compensate for this unwanted development, novel antimicrobial drugs are required. Therefore, insights into essential processes in the cell, such as chromosome segregation, could potentially lead to the identification of new drug targets and to the development of novel antimicrobials. In the current study we aimed to get a first glimpse of the molecular mechanisms underlying chromosome segregation in *S. pneumoniae*.

Eubacterial chromosomes contain a single origin of replication (*oriC*) that is recognized by the initiator protein DnaA that allows assembly of a replication initiation complex and mediates open complex formation (Kornberg and Baker, 1992; Mott and Berger, 2007; Zakrzewska-Czerwinska *et al*., 2007; Katayama *et al*., 2010; Scholefield *et al*., 2011). Daughter chromosomes produced by DNA replication must be segregated to opposite halves of the cell so that after cell division both daughter cells inherit a single copy of the chromosome (Reyes-Lamothe *et al*., 2008; Graumann and Knust, 2009; Bloom and Joglekar, 2010; Errington, 2010; Toro and Shapiro, 2010). The processes underlying chromosome segregation in bacteria are still poorly understood. Nevertheless, work in model organisms such as *Bacillus subtilis*, *Caulobacter crescentus* and *Escherichia coli* have revealed two key players; the chromosome partitioning system, ParABS and the SMC (structural maintenance of chromosomes) protein complex (Thanbichler, 2009; Gerdes *et al*., 2010; Toro and Shapiro, 2010).

The ParABS locus is a widely conserved system that was originally identified as a crucial factor for the partitioning of low-copy number plasmids (Ringgaard *et al*., 2009; Gerdes *et al*., 2010; Salje, 2010). Recently, it has been demonstrated that chromosomally encoded ParABS loci also play important roles in the segregation of sister DNA molecules. *parA* and *parB* genes as well as *parS* sites, to which ParB proteins specifically bind, are generally found organized as operons in close proximity to *oriC* (Livny *et al*., 2007). ParA proteins are Walker-type ATPases that have been shown in *Vibrio cholerae* and *C. crescentus* to form filaments within the cell that possibly extend from one cell pole to the vicinity of one *oriC* region

Accepted 26 May, 2011. For correspondence. *E-mail j.w.veening@rug.nl; Tel. (+31) 50 363 2408; Fax (+31) 50 363 2348; **E-mail sgruber@biochem.mpg.de; Tel. (+49) 89 8578 3440; Fax (+49) 89 8578 3430. †Both authors contributed equally.

of the chromosome (Fogel and Waldor, 2006; Hui *et al*., 2010; Ptacin *et al*., 2010; Schofield *et al*., 2010). ParB–*parS* nucleoprotein complexes located near *oriC* are thought to induce ATP hydrolysis by ParA proteins thereby pulling the *oriC* region of the chromosome towards the cell pole. ParA in *B. subtilis* (also) regulates the initiation of chromosomal DNA replication via DnaA (Murray and Errington, 2008). Interestingly, the genomes of some organisms, including *S. pneumoniae*, lack *parA* (but not *parB*) homologues, suggesting that they have lost the chromosome segregation activity of the *parABS* system. This raises the question which alternative mechanisms ensure proper separation of sister chromosomes in these organisms.

In eukaryotes, the maintenance of chromosomes depends on several SMC complexes that function in diverse processes such as sister chromatid cohesion, recombination, DNA repair and mitotic chromosome condensation (Onn *et al*., 2008; Hudson *et al*., 2009; Nasmyth and Haering, 2009). Bacteria encode only a single highly conserved SMC protein that forms complexes with ScpA and ScpB proteins, the former being a member of the kleisin family of proteins. The genomes of some γ-proteobacteria (e.g. *E. coli*) lack SMC and ScpAB homologues but encode for structurally related proteins called MukB and MukEF. The precise function of bacterial SMC complexes is still unclear; however, they have been suggested to play a crucial role in the organization and condensation of chromosomes (Mascarenhas *et al*., 2002; Gruber and Errington, 2009; Sullivan *et al*., 2009).

Both SMC-ScpAB in *B. subtilis* and MukBEF in *E. coli* form discrete foci in the cell that localize in the vicinity of the origin of replication (Danilova *et al*., 2007). In *B. subtilis*, this chromosomal localization of condensin depends on ParB proteins bound to *parS* sites (Gruber and Errington, 2009; Sullivan *et al*., 2009). Deletions of genes of the SMC complex in *B. subtilis* result in strains with a lethal phenotype at standard growth conditions. At slow growth, these strains show aberrant chromosome structures and contain a high proportion of anucleate cells indicating a role in chromosome segregation (Britton *et al*., 1998; Moriya *et al*., 1998; Mascarenhas *et al*., 2002; Soppa *et al*., 2002). However, in *Mycobacterium smegmatis* and spherical organisms like *Staphylococcus aureus* and *Deinococcus radiodurans* it has been reported that *smc* deletion mutants grow normally with only minor phenotypic aberrations, such as a few anucleated cells or hypersensitivity to gyrase inhibiting drugs (Guthlein *et al*., 2008; Bouthier de la Tour *et al*., 2009; Yu *et al*., 2010).

Little is known about chromosome segregation in *Streptococci*, a taxonomic group belonging to the firmicutes and comprising major pathogens such as *S. pneumoniae*. However, the presence of *parB* in *S. pneumoniae* was identified previously (Gasc *et al*., 1997; Halfmann *et al*., 2007) and *smc* was properly annotated in the *S. pneumoniae* genome sequence (Hoskins *et al*., 2001; Lanie *et al*., 2007). Therefore, we hypothesized that the ParB/*parS*/SMC segregation system is also important for chromosome segregation in *S. pneumoniae*. We tested this hypothesis using a combination of fluorescence microscopy and chromatin immunoprecipitation (ChIP) techniques and we show that indeed also the pneumococcal homologue of ParB is enriched at *parS* sites near *oriC*. We confirm that the previously predicted *parS* sites are functional (Livny *et al*., 2007), and identify a fourth *parS* site to which ParB accumulates at high levels. Furthermore, we show that *S. pneumoniae* SMC is recruited to *parS* by the action of ParB. Moreover, we demonstrate that ParB is not essential in *S. pneumoniae* although a *parB* mutant exhibits mild defects in chromosome segregation. Finally, we managed to obtain a *smc* deletion mutant, which is viable although this strain also displays deficits in chromosome segregation. Taken together, our data suggest a similarity between the mechanisms found in *B. subtilis* and *S. pneumoniae* although other, not yet identified, mechanisms also play a role in chromosome organization and segregation in *S. pneumoniae*.

Results

ParB protein accumulates at parS *sites near the origin of replication region*

For *B. subtilis* it was previously shown that ParB (Spo0J) fused to the green fluorescent protein (GFP) forms discrete foci within a cell when examined by fluorescence microscopy, and that the location of the foci correspond to origin regions (Glaser *et al*., 1997; Lin *et al*., 1997; Sullivan *et al*., 2009). In order to visualize the localization of *S. pneumoniae* ParB in living cells, a C-terminal GFP fusion was constructed that contains *parB* fused to the *gfp* gene at its endogenous locus under its own promoter thereby replacing the wild-type *parB* gene (strain MT2, Fig. 1A). The ParB–GFP construct appears to be fully functional, as judged by growth curve analysis (see below; Fig. S1), and by the absence of aberrantly shaped cells (data not shown). Cells were grown in C+Y medium at 30°C and fluorescence microscopy of the cells showed foci (up to 2 discrete foci per cell) but also a cytoplasmic/nucleoid signal (Fig. 1B), which was not present in an untagged control (data not shown). Western blot analysis showed that this cytoplasmic signal was not due to degradation of ParB–GFP (Fig. 1C). Staining of the DNA with DAPI (4′-6-diamidino-2-phenylindole) showed that the foci overlap with the nucleoid (data not shown).

To define whether and at which location(s) ParB binds to the chromosome, a ChIP experiment in combination

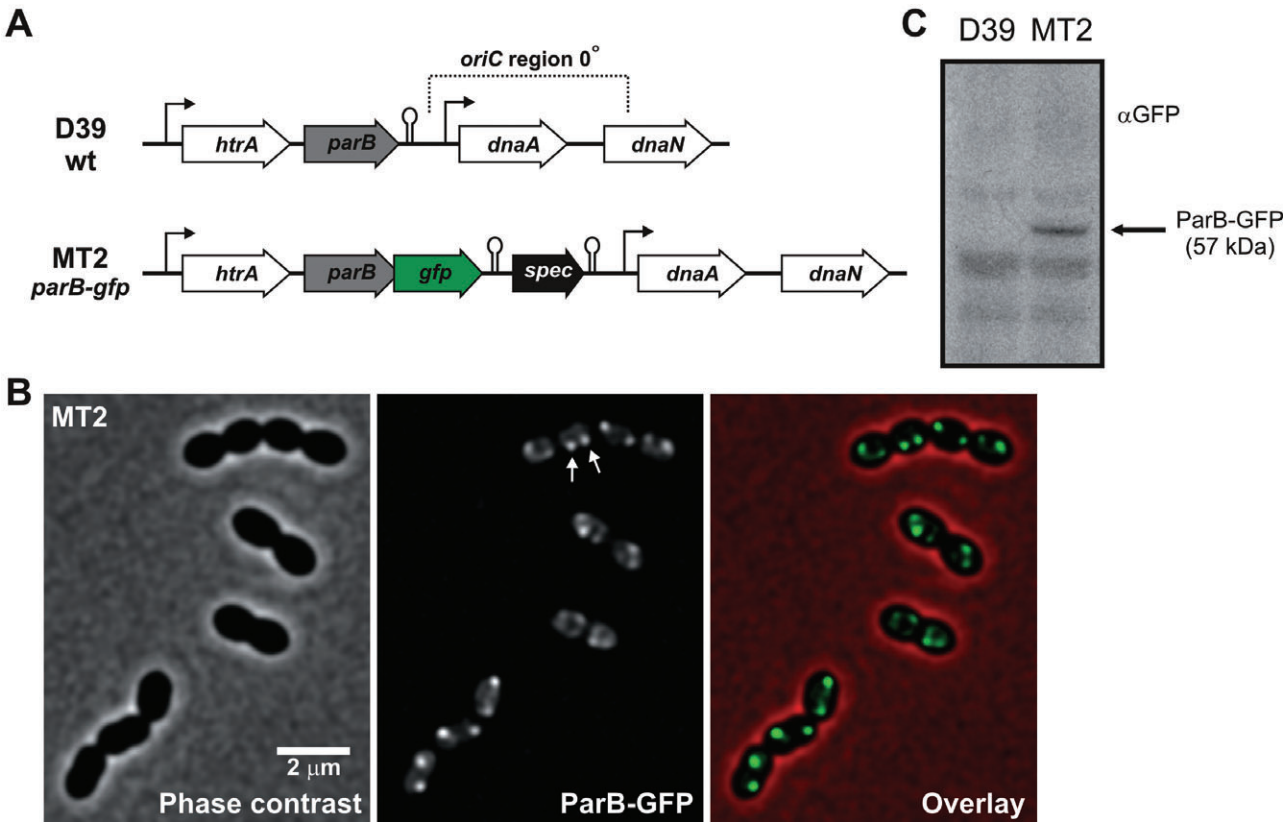

Fig. 1. ParB–GFP localizes as foci in live cells.
A. Schematic presentation of the *parB* locus, which is near *oriC*, and the genetic layout of strain MT2 in which the native *parB* gene is replaced by a *parB–gfp* fusion. The *oriC* region (0° of the circular chromosome) is indicated by a dotted line.
B. Localization of ParB–GFP in live *S. pneumoniae* cells. Micrographs of strain MT2 (P_{parB}-*parB–gfp*) are shown. Arrows indicate a ParB–GFP focus.
C. Western blot analysis of strains D39 and MT2.

with hybridization to a high-density amplicon array (ChIP-on-chip) was performed utilizing the ParB–GFP strain (MT2). Cells were grown to exponential phase in GM17 medium at 37°C, fixed with formaldehyde, and subjected to ChIP using GFP-specific antibodies coupled to magnetic beads (for details see *Experimental procedures*). DNA from the input and eluate fractions was randomly amplified, labelled and hybridized to a DNA-microarray. The ratio of intensities between eluate and input DNA was plotted against the position on the chromosome. As shown in Fig. 2A, ParB–GFP is particularly enriched in the vicinity of the *oriC* region. Furthermore, the three *parS* sites previously predicted by bioinformatics at 2° (at ~ 11 kb of the 2046 kb *S. pneumoniae* D39 genome), –3.7° (2025 kb) and –19.2° (1936 kb) from *oriC* (Livny *et al*., 2007) all show a high ParB–GFP enrichment. Strikingly, the highest accumulation of ParB–GFP was observed for probe SPD_2057 at approximately –2° (2036 kb) from *oriC* (Fig. 2A). In an attempt to identify whether a putative *parS* site is present at this location, we used the predicted *S. pneumoniae parS* site that scored the highest according to the algorithm of Livny *et al*. 2007 (*parS* at 2° from *oriC*: 5′-TGTTTCACGTGAAACA-3′) and searched the *S. pneumoniae* D39 genome for similar sequences with either 1 or 2 mismatches using the genome mining software Genome2D (Baerends *et al*., 2004). Our search identified four sequences, three of which, not surprisingly, were also the predicted *parS* sites by Livny *et al*. The fourth motif however had the sequence 5′-AGTTTCACGTGAAACT-3′ (a perfect 8 bp inverted repeat with two changes compared with *parS* at 2°) and was located at –1.6° from *oriC*, almost exactly where the ChIP-chip data showed the highest enrichment of ParB–GFP. A high level of ParB–GFP enrichment was also observed for probe SPD_1620, at approximately –72° (1635 kb) from *oriC* (Fig. 2A). Our bioinformatics analysis, however, failed to find a clear *parS* consensus sequence at this site. Some minor sites of enrichment were also observed, for instance, at approximately –29° and 6° from *oriC* (Fig. 2A), but also at these sites sequences with close homology to the *parS* consensus could not be identified.

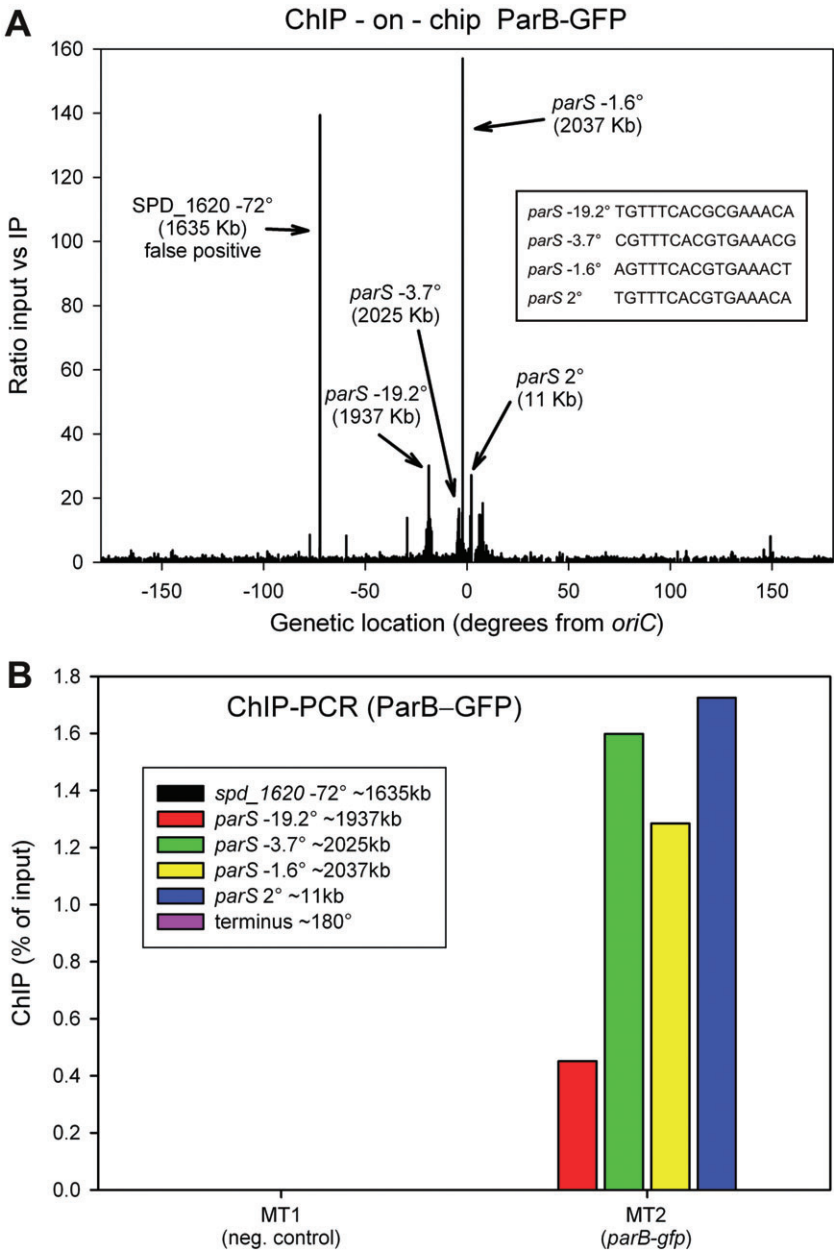

Fig. 2. ParB is enriched at *parS* sites near the origin of replication.
A. ChIP-on-chip analysis of the distribution of ParB–GFP on the *Streptococcus pneumoniae* genome. Exponentially growing cells of strain MT2 (ParB–GFP) were subjected to chromatin immunoprecipitation (ChIP) using anti-GFP antibodies and microarray analysis (chip). Enrichment in the eluate immunoprecipitated (IP) fraction relative to the input DNA sample is shown for the length of the circular chromosome starting with the terminus of replication (–180° from *oriC*). The positions of *parS* sites are indicated as well as the false positive probe SPD_1620.
B. Exponentially growing cells of strains MT1 (*parB–spec*) and MT2 (*parB–gfp–spec*) were collected for ChIP analysis using anti-GFP antibodies. Input and eluate DNA samples were analysed by real-time quantitative PCR. Pull-down efficiency (ChIP-DNA/input-DNA*100) is plotted for each primer pair. A typical outcome of a ChIP-qPCR experiment is shown.

To verify the ChIP-chip data, the DNA of the input and eluate fractions of strains MT1 (no GFP, negative control) and MT2 (ParB–GFP) were analysed using real-time quantitative PCR with primer pairs specific for the three previously predicted *parS* sites (2°, –3.7° and –19.2°), the newly identified *parS* site (–1.6°), probe SPD_1620 (–72°) and the terminus of replication. From the strain lacking GFP (MT1) very little DNA was precipitated (not visible due to the scale of the graph). In contrast, the four *parS* sites of strain MT2 (ParB–GFP) were pulled down efficiently (Fig. 2B). ParB–GFP was not enriched at SPD_1620 (–72°), indicating that the ChIP-chip peak for SPD_1620 constitutes a microarray artefact. As expected, ParB–GFP was also not enriched at the terminus region. Taken together, these data show that *S. pneumoniae* contains at least four *parS* sites that are all highly occupied by ParB *in vivo*.

ParB recruits SMC to parS *sites*

Based on prior studies in *B. subtilis* and the results described above, we hypothesized that *S. pneumoniae* ParB recruits the SMC complex to the *oriC* region. To test this hypothesis *in vivo,* we set out to generate a fusion of SMC to GFP at its endogenous locus under its own promoter. Unfortunately, construction of a SMC–GFP

fusion at its endogenous locus failed in several attempts. Therefore, we constructed an N-terminal fusion of GFP to SMC (strain AM14) utilizing the vector pJWV25, which places the gene fusion under the control of a zinc-inducible promoter (P_{Zn}) and integrates the construct at the non-essential *bgaA* locus leaving the endogenous *smc* locus intact (Eberhardt *et al*., 2009) (Fig. S2A). The GFP–SMC fusion is functional since it is able to restore normal growth in *smc* mutant cells (see below; Fig. S2C–D). Strains D39 (wild-type) and AM14 (GFP–SMC) were grown in C+Y medium at 30°C and at mid-exponential growth, 0.15 mM $ZnSO_4$ was added and cells were analysed by Western blotting (Fig. S2B) and fluorescence microscopy after 1 h of induction. As shown in Fig. 3A, a nucleoid-like localization was observed with the frequent presence of distinct foci in most cells (on average 0.73 foci per cell, 562 cells counted). Since SMC colocalizes with ScpB in *B. subtilis* (Mascarenhas *et al*., 2002) we examined localization of the pneumococcal homoloque of ScpB. As shown in Fig. S3A, GFP–ScpB displays a nucleoid-like localization with the clear presence of foci, very similar to the localization pattern of GFP–SMC.

If ParB is responsible for the recruitment of the SMC complex to the *parS* sites and the foci observed for strain AM14 (GFP–SMC) represent localization of GFP–SMC at the *parS* sites, then the foci should disappear in the absence of ParB. Therefore, we constructed a *parB* deletion strain (see below) and introduced this construct into the GFP–SMC reporter strain, resulting in strain AM16 (*gfp–smc*, Δ*parB*). Strikingly, GFP–SMC foci were rarely observed in the absence of ParB (Fig. 3B) (on average 0.09 foci per cell, 514 cells counted). As only a small level of protein degradation was present for the GFP strains, most of the observed fluorescence signal reflects full-length GFP–SMC (Fig. S2B). GFP–ScpB foci were also absent when *parB* was deleted (Fig. S3B). It should also be noted that the fluorescence signals were not uniform in all cells, which is likely due to the inducible system used and the relatively short induction time.

To verify these microscopic observations, we attempted to detect specific accumulation of SMC at *parS* sites by ChIP. Using GFP-specific antibodies, we performed ChIP on exponentially growing cells of strains AM10 (*gfp*, negative control), AM14 (*gfp–smc*) and AM16 (*gfp–smc*, Δ*parB*) with primer pairs specific for the four *parS* sites, the terminus of replication (Fig. S4), and for multiple other chromosomal locations on both the left and right arms of the chromosome (Fig. 3C). The DNA of the input and eluate fractions were analysed using real-time quantitative PCR. As expected, the control strain carrying an untagged GFP (AM10) showed low levels of enrichment at all tested genetic loci (Fig. S4). Strain AM14 (GFP–SMC) however, showed strong enrichment at multiple positions within a 50kb region around *oriC* that includes the three *parS* sites with highest ParB occupancy (*parS* –3.7°, *parS* –1.6° and *parS* 2°) (Fig. 3C). Much less SMC was detected by ChIP at fifteen other sites on the left and right arm of the chromosome and the replicaton terminus region. In accordance with the microscopy data, in the absence of ParB protein, the strong enrichment of GFP–SMC near *oriC* was lost and the protein was instead nearly uniformly distributed over the tested genetic loci (Fig. 3C and Fig. S4). This suggests that ParB is crucial for the recruitment of SMC to the origin of replication region in *S. pneumoniae*.

ParB contributes to chromosome segregation but is not essential in S. pneumoniae

Although a knock-out of *parB* in *S. pneumoniae* has been reported previously (Δ*spoJ*::*ermAM*), this mutant has not been studied with regard to chromosome segregation (Sebert *et al*., 2002). Furthermore, Dagkessamanskaia and co-workers constructed a strain that lacked the upstream regulatory region of *parB* (Δ*htrA-orfL*) likely resulting in transcriptional downregulation of *parB*, but this strain was studied in the context of genetic competence (Dagkessamanskaia *et al*., 2004). In order to investigate the role of *parB* in *S. pneumoniae* in the context of chromosome segregation, we constructed a complete, non-polar deletion of *parB* (Fig. 4A and see *Experimental procedures*) and sequencing verified the *parB* locus in the mutant. The growth rate of the *S. pneumoniae parB* deletion mutant in exponential phase is similar to wild-type; however a slight increase in the lag phase after dilution of exponentially growing cells was consistently observed (Fig. 4C and Fig. S1). Cell viability, as determined by plating assays, showed no significant difference compared with wild-type (Fig. S5).

To examine whether ParB plays a role in chromosome segregation, DNA of exponential growing cells from C+Y medium at 30°C was stained with DAPI and cells were analysed by phase-contrast and fluorescence microscopy. In the wild-type (MT1) no cells lacking nucleoids (0 out of 1000) were observed whereas in the Δ*parB* mutant 0.8% (8 out of 950) of the cells were anucleate (significantly different from the wild-type, $P < 0.05$, Fisher's exact test). This percentage is comparable with the phenotype observed for a *parB* deletion mutant in *B. subtilis* where 1% to 2% anucleate cells were observed (Ireton *et al*., 1994). When cells were grown at 37°C, the chromosome segregation defect was even more severe (3.5% anucleate cells, 42 out of 1210 cells, $P < 0.05$, Fisher's exact test) and besides anucleate cells, frequently cells with unseparated nucleoids were observed (Fig. 5A and B). Taken together, these results indicate that ParB is essential for efficient chromosome segregation in *S. pneumoniae*.

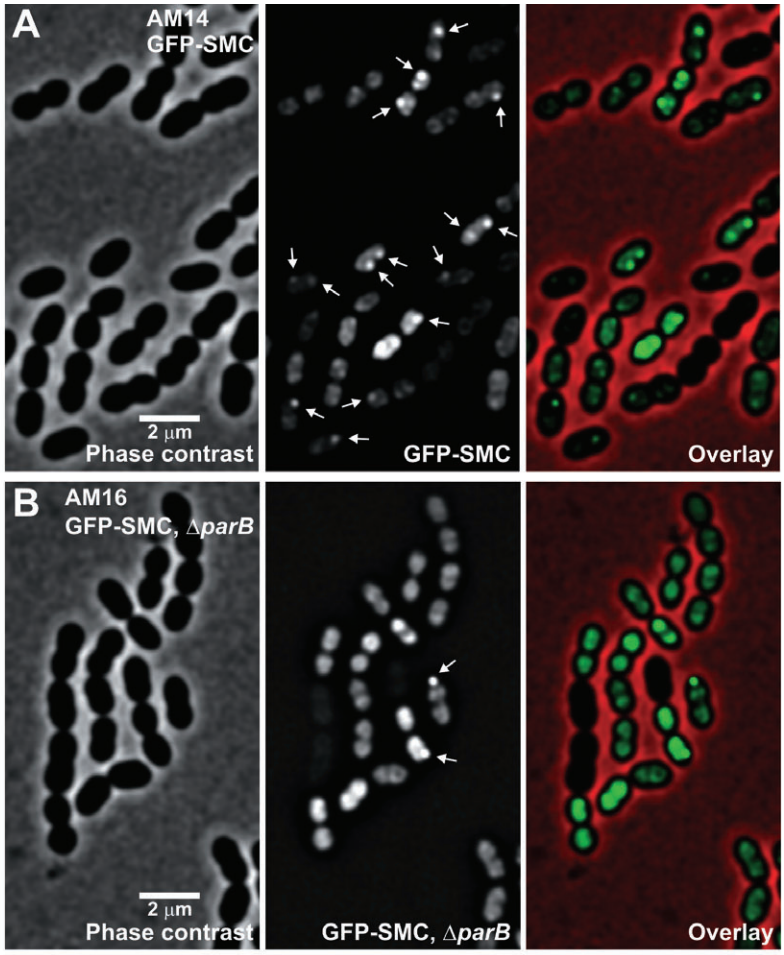

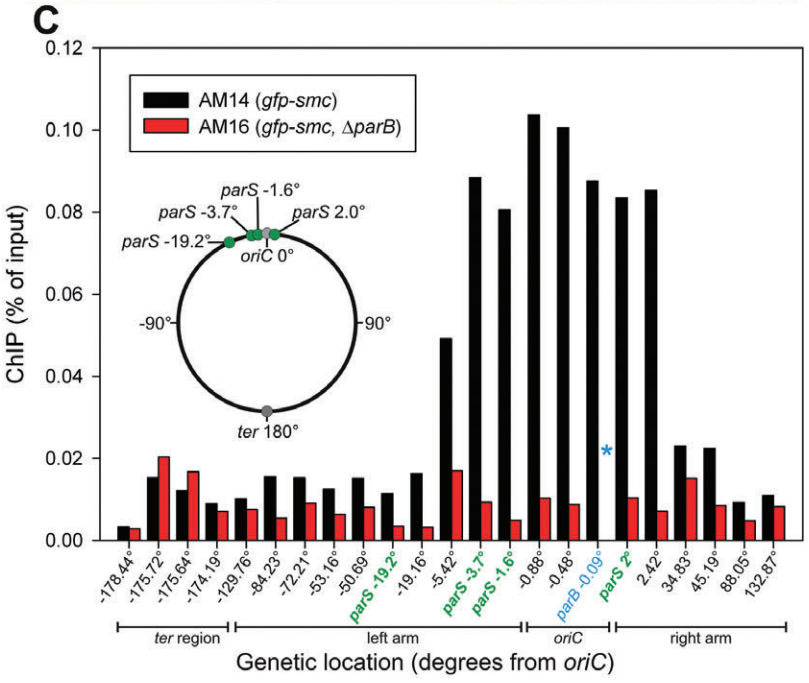

Fig. 3. Localization of SMC depends on ParB. Cells were analysed by fluorescence microscopy as described in the *Experimental procedures*. Micrographs of strains AM14 (P_{Zn}–*gfp–smc*) (A) and AM16 (P_{Zn}–*gfp–smc*, Δ*parB*) (B) are shown. Arrows indicate GFP–SMC foci.
C. ChIP-qPCR analysis shows that GFP–SMC is specifically enriched near *oriC*, only in the presence of ParB. Pull-down efficiency for strains AM14 and AM16 (ChIP-DNA/input-DNA*100) is plotted for each primer pair. A typical outcome of a ChIP-qPCR experiment is shown. The asterisk (*) indicates that the qPCR primer pair for the *parB* locus does not amplify DNA in the *parB* mutant strain AM16.

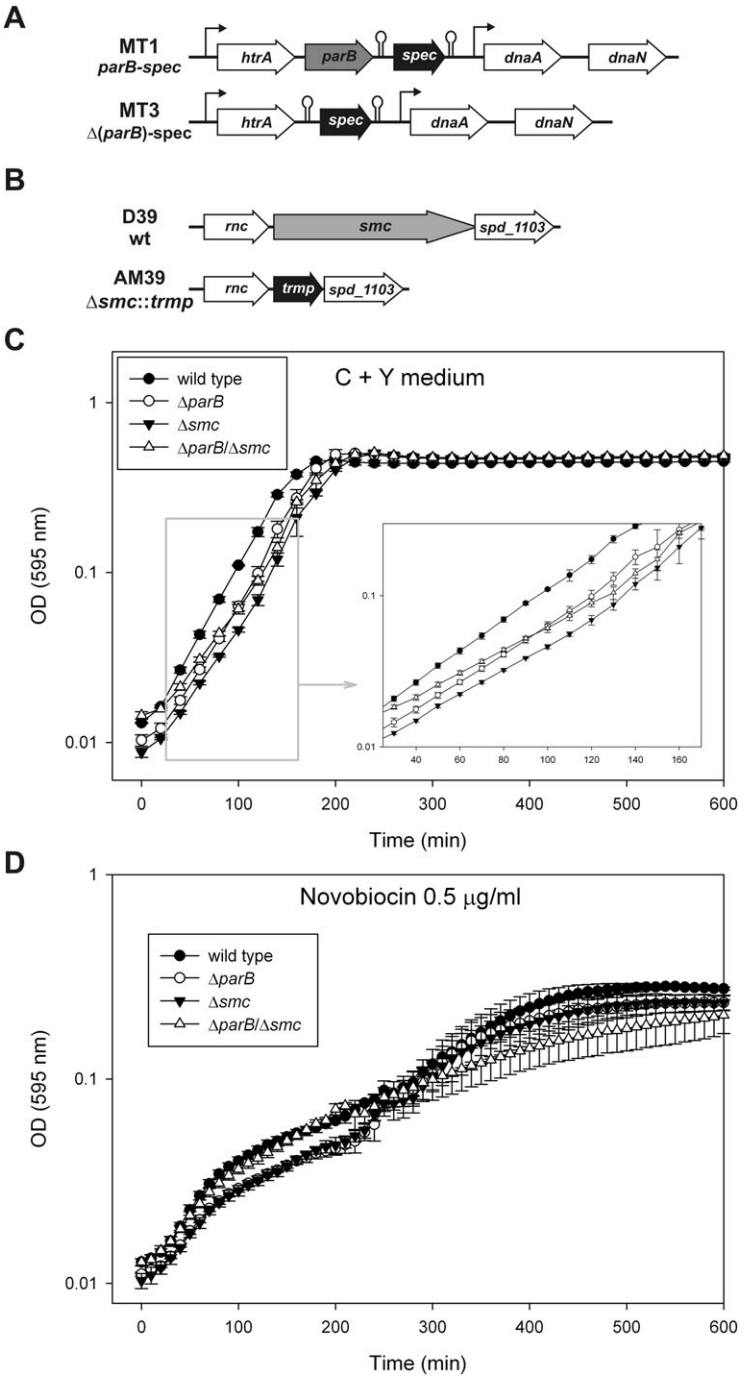

Fig. 4. Growth analysis of cells lacking ParB and SMC.
A. Schematic presentation of the *parB* locus and the genetic layout of strains MT1 and MT3. Strain MT1 contains a spectinomycin inserted downstream of the *parB* gene, leaving the *parB* and *oriC* loci intact. DNA of strain MT1 was used as a template to construct strain MT3, in which *parB* is completely removed (see online supplementary information for more details).
B. Schematic presentation of the *smc* locus and the genetic layout of strain AM39 (Δ*smc*). Strain AM39 was constructed by replacing the entire *smc* gene with a promoterless and terminatorless trimethoprim resistance cassette, leaving the rest of the operon intact (also see Fig. S6).
C. Cells were grown in C+Y medium at 37°C in microtitre plates and the OD_{595} was measured every 10 min (log scale). Error bars show the standard deviation between at least 3 independent growth curves. The inset show the time between 30 and 170 min.
D. *parB* and *smc* mutants are not hypersensitive to gyrase inhibitors. Cells were grown as above but in the presence of 0.5 μg ml^{-1} of novobiocin.

SMC is not essential in S. pneumoniae *but shows defects in chromosome segregation*

In many bacteria the deletion of the *smc* gene results in impaired growth and other phenotypes. For instance, in *B. subtilis* a *smc* deletion mutant cannot grow at high growth rates, and anucleate cells are frequently observed even under slow growth conditions (Britton *et al*., 1998; Britton *et al*., 1998; Moriya *et al*., 1998; Moriya *et al*., 1998; Mascarenhas *et al*., 2002; Soppa *et al*., 2002). Moreover, a *B. subtilis smc* mutant is hypersensitive to gyrase inhibiting drugs (Lindow *et al*., 2002). It has recently been shown that *smc* deletion mutants in cocci, such as *S. aureus* and *D. radiodurans*, grow normally with only mild phenotypes (Bouthier de la Tour *et al*., 2009; Yu *et al*., 2010).

The abovementioned observations in rod-shaped and round cells made us wonder if the oval-shaped *S. pneu-*

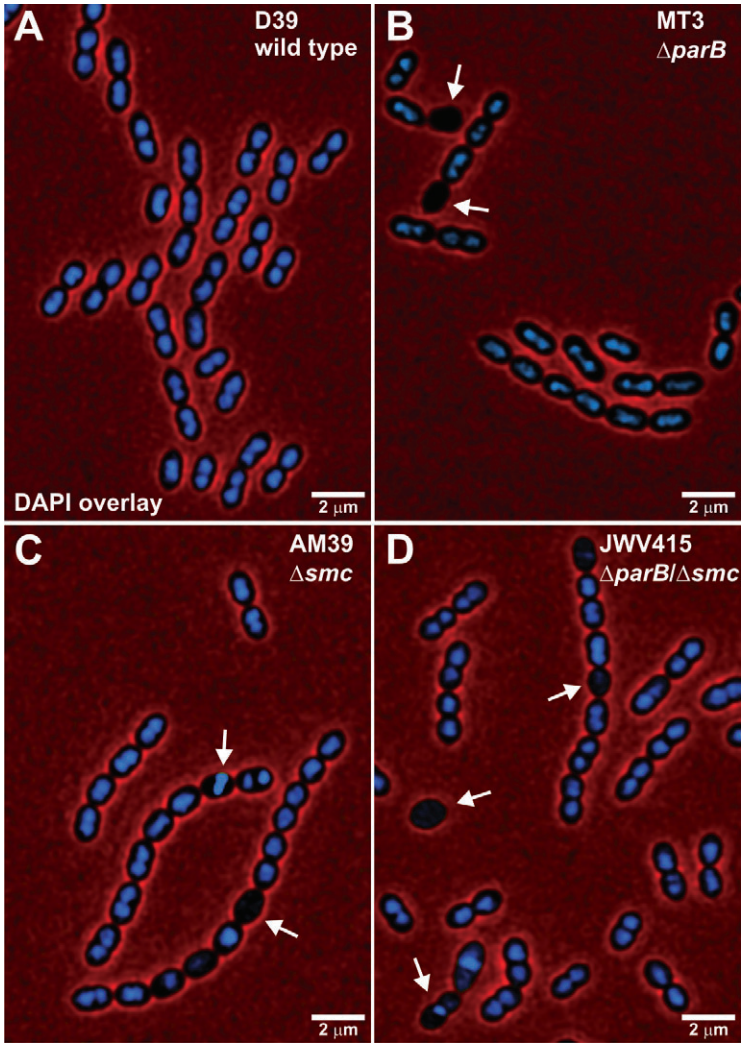

Fig. 5. ParB and SMC are required for efficient chromosome segregation. Cells were grown in C+Y medium at 37°C and the DNA was stained with DAPI and collected for fluorescence microscopy. Overlays between phase-contrast (red signal) and DAPI fluorescence (blue signal) are shown. Arrows indicate anucleate or abnormal cells. Micrographs of strain D39 (wild-type) (A), strain MT3 (Δ*parB*) (B), strain AM39 (Δ*smc*) (C) and strain JWV415 (Δ*parB*/Δ*smc*) (D) are shown.

moniae would be viable without *smc* and what phenotypic aberrations *smc* mutants would generate. We managed to construct a *smc* deletion mutant by replacing the endogenous *smc* gene with a trimethoprim resistance cassette (Fig. 4B and see *Experimental procedures*). Southern blotting, PCR and sequencing verified the successful construction of the *smc* replacement mutant, thus *smc* is not essential in *S. pneumoniae* (Fig. S6). Investigating growth revealed that the Δ*smc* mutant displays growth characteristics very similar to the Δ*parB* mutant, and although the growth rate and cell viability is comparable to the wild-type, Δ*smc* cells show a prolonged lag phase (Fig. 4C and Fig. S5). Importantly, DAPI staining showed 0.5% (5 out of 950) anucleate cells in the Δ*smc* mutant when grown at 30°C in C+Y medium (significantly different from wild-type, $P < 0.05$, Fisher's exact test). The chromosome segregation phenotype was exacerbated when cells were grown at 37°C (1.8% anucleate cells, 17 out of 965 cells counted, $P < 0.05$, Fisher's exact test, Fig. 5C). Interestingly, the Δ*smc*/Δ*parB* double mutant displayed a phenotype similar to the individual knockouts at 37°C (2.8% anucleate cells, 39 out of 1408 cells; not significantly different from the Δ*parB* or the Δ*smc* mutants, Fisher's exact test $P = 0.31$ and $P = 0.13$ respectively) (Fig. 5D and Fig. S5).

To test whether the *S. pneumoniae* Δ*smc* mutant, the Δ*parB* mutant or the Δ*smc*/Δ*parB* double mutant are hypersensitive to gyrase inhibiting drugs, we grew cells of strains D39 (wild-type), AM39 (Δ*smc*), MT3 (Δ*parB*) and JWV415 (Δ*smc*, Δ*parB*) in C+Y medium in microtitre plates containing different concentrations of antibiotics. We not only tested the gyrase inhibitor novobiocin (Ferrandiz *et al*., 2010), but also examined growth at sub-inhibitory concentrations of norfloxacin and ciprofloxacin (both targeting topoisomerases) and ampicillin (targeting penicillin binding proteins). As shown in Fig. 4D, a hypersensitive response to the gyrase inhibitor novobiocin, or any of the other antibiotics could not be observed (Fig. S7A–C). The mutants also did not demonstrate a temperature-sensitive growth phenotype (Fig. S7D).

Discussion

The conserved *parABS* module has at least three independent functions in the maintenance of bacterial chromosomes: (i) it promotes the segregation of replicated chromosomes as shown in *V. cholera* and *C. crescentus* presumably by pulling *oriC* regions towards the cell poles (Ptacin *et al*., 2010; Schofield *et al*., 2010; Fogel and Waldor, 2006); (ii) it regulates the timing of initiation of DNA replication presumably by a direct interaction of ParA with the replication initiation protein, DnaA, at least in *B. subtilis* (Murray and Errington, 2008) and (iii) it recruits the SMC protein complex to the vicinity of the origin of replication in *B. subtilis* (Gruber and Errington, 2009; Sullivan *et al*., 2009) and as well as in *S. pneumoniae* (this work). The latter function of *parABS* is completely independent of ParA protein as the genome of *S. pneumoniae* lacks any ParA protein homologues. Thus, *S. pneumoniae* appears to have lost the two ParA dependent functions of the *parABS* module but retained its activity for the recruitment of condensin to replication origins.

By deleting *parB* in *S. pneumoniae* we found strong indications that pneumococcal ParB is indeed involved in chromosome segregation because of a significant proportion of anucleate cells (Fig. 5). The fact that *smc* and *smc*/*parB* double mutants have similar phenotypes is consistent with the notion that recruitment of SMC to the chromosome is a main function of ParB protein in *S. pneumoniae*. Interestingly, *S. pneumoniae* ParB was shown to interact with the cell division protein DivIVA in a bacterial two-hybrid screen and by co-immunoprecipitation experiments, suggesting that ParB might also be important in connecting the process of chromosome segregation with cell division (Fadda *et al*., 2007). Whether the DivIVA–ParB interaction is relevant *in vivo* remains to be tested.

In *B. subtilis* a *smc* deletion mutant is only viable under slow growth conditions (Britton *et al*., 1998; Moriya *et al*., 1998). Strikingly, we managed to construct a *smc* deletion mutant in *S. pneumoniae* which is viable in normal growth media and at normal or even elevated temperatures and is not hypersensitive to a number of antibiotics including novobiocin, a potent gyrase inhibitor (Fig. 4, Figs S5 and S7). However, the Δ*smc* mutant does show a significant proportion of anucleate cells indicating an important role of SMC for efficient chromosome segregation (Fig. 5).

Taken together, our results show that *S. pneumoniae* contains a functional chromosome segregation machine that promotes efficient chromosome segregation by recruitment of SMC via ParB. The ChIP data shows that while ParB is specifically enriched at *parS* sites (Fig. 2), SMC is more widely distributed over the chromosome with a strong enrichment in a large region (~ 50 kb) around *oriC* (Fig. 3C). This is also consistent with the microscopy data that show that GFP–SMC foci are a bit more diffuse and were more difficult to capture than ParB–GFP foci. The frequent observation of two connected daughter cells that contain a bilobed nucleoid in the *parB*/*smc* mutants, suggests that a major role of ParB and SMC is to facilitate the partitioning of chromosomes (Fig. 5). This first in-depth analysis of the ParB/*parS*/SMC system in a Gram-positive organism other than *B. subtilis* suggests that the ParB/*parS*/SMC system might be a mechanism that ensures efficient chromosome segregation in a wide variety of bacteria.

While the ParB/*parS*/SMC system seems to be similar between the two organisms, it remains puzzling why SMC and ParB are not essential in *S. pneumoniae* under laboratory conditions. An attractive hypothesis is that *S. pneumoniae* contains additional, as of yet unknown chromosome segregation factor(s) that drive this process. An alternative hypothesis is that chromosome segregation in *S. pneumoniae* occurs rather passively via an entropy driven process in which the role of proteins such as SMC is to create the right physical conditions that support self-demixing of sister chromosomes (Jun and Mulder, 2006; Jun and Wright, 2010). These exciting hypotheses are currently under investigation in our laboratories and might result in the identification of novel targets that could be used to combat pathogenic *Streptococci*.

Experimental procedures

Strains, plasmids and growth conditions

Bacterial strains and plasmids used in this study are listed in Table 1. *S. pneumoniae* strains were grown as standing cultures in M17 broth (Terzaghi and Sandine, 1975) containing 0.5% (w/v) glucose (GM17) (for ChIP analysis) or in complex C+Y medium (Martin *et al*., 1995) at 30°C or 37°C (for microscopy). Detailed growth conditions are described in the supplementary information as well as the construction of the plasmids and strains used.

Recombinant DNA techniques and oligonucleotides

Procedures for DNA purification, restriction, ligation, agarose gel electrophoreses and transformation of *E. coli* were carried out as described by (Sambrook, 2001). The oligonucleotides used in this study are listed in Table S1 and were obtained from Biolegio (Nl). *S. pneumoniae* chromosomal DNA was isolated using a Promega Wizard Genomic DNA Purification Kit. DNA modifying enzymes were purchased from Roche (Mannheim, Germany), New England Biolabs (Ipswich, USA), Bioline (London, UK) and Fermentas (Burlington, Canada) and used as described by the manufacturer.

Growth curves

Growth curves were performed in 96 wells plate in a microtitre plate reader (Tecan Infinite F200 pro), cells were grown at 37°C and OD_{595} was measured every 10 or 15 min.

Table 1. Plasmids and bacterial strains used in this study.

Strain/plasmid	Relevant genotype[a]	Reference
E. coli		
EC1000	F⁻, *araD139* (*ara ABC-leu*)*7679*, *galU*, *galK*, *lacX74*, *rspL*, *thi*, *repA* of pWV01 in *glgB*, Km^R	Leenhouts *et al.* (1996)
S. pneumoniae		
D39	Serotype 2 strain, *cps2*	Avery *et al.* (1944)
MT1	D39, *parB–spec* (*spec* integrated just after *parB* locus)	This study
MT2	D39, *parB–gfp–spec*	This study
MT3	D39, Δ(*parB*)*–spec* (*parB* deleted, *spec* integrated just after *parB* locus)	This study
AM10	D39, *tet, bgaA*::P_{Zn}*–gfp*	This study
AM13	D39, *tet, bgaA*::P_{Zn}*–gfp–scpB*	This study
AM14	D39, *tet, bgaA*::P_{Zn}*–gfp–smc*	This study
AM15	D39, *tet, bgaA*::P_{Zn}*–gfp–scpB*, Δ(*parB*)*–spec*	This study
AM16	D39, *tet, bgaA*::P_{Zn}*–gfp–smc*, Δ(*parB*)*–spec*	This study
AM39	D39, Δ*smc*::*trmp* (*smc* replaced by *trmp*)	This study
JWV415	D39, Δ*smc*::*trmp*, Δ(*parB*)*–spec*	This study
Plasmids		
pKOT	*amp*, *trmp*, *pBluescript II KS+*	Hendriksen *et al.* (2008)
pORI38	*spec*, *ori*⁺ *repA*⁻	Leenhouts *et al.* (1996)
pJWV25	*amp*, *bgaA′*, *tet*, P_{Zn}*–gfp*, *′bgaA*	Eberhardt *et al.* (2009)
pAM6	*amp*, *bgaA′*, *tet*, P_{Zn}*–gfp–smc*, *′bgaA*	This study
pAM9	*amp*, *bgaA′*, *tet*, P_{Zn}*–gfp–scpB*, *′bgaA*	This study

a. Km^R, kanamycin resistant; *spec*, spectinomycin resistance marker; *tet*, tetracycline resistance marker; *amp*, ampicillin resistance marker; *trmp*, trimethoprim resistance marker.

Western blot analysis and immunodetection

Cells were grown in C+Y medium (4 ml) with or without 0.15 mM $ZnSO_4$ and were harvested at an OD_{600} of approximately 0.3 by centrifugation at 9000 r.p.m. for 5 min. The pellet was resuspended in 100 µl of SEDS lysis buffer and cells were incubated for 5 min at 37°C. Samples were diluted in 100 µl 2× SDS-loading buffer, boiled for 5 min at 100°C and separated by SDS-polyacrylamide gel electrophoresis (SDS-PAGE). Next, proteins were transferred to a polyvinylidene difluoride (PVDF) membrane as described (Sambrook, 2001). ParB–GFP and GFP–SMC were detected with polyclonal anti-GFP antibodies (Invitrogen) and anti-IgG-rabbit-HRP antibody (GE Healthcare) according to the manufacturer's instructions.

Fluorescence microscopy

Cells were grown at 30°C (or at 37°C for strains AM13 and AM15) in plastic 5 ml capped tubes, filled to a maximum of 3 ml to allow for enough air for proper GFP folding, basically as described previously (Eberhardt *et al.*, 2009). Microscopy pictures were taken with a Deltavision (Applied Precision) IX71 Microscope (Olympus), using a CoolSNAP HQ2 camera (Princeton Instruments) and a 300W Xenon light source through a 100× oil immersion objective (phase contrast). For more details, see the supplementary information.

Chromatin immunoprecipitation (ChIP)

Cells were grown to mid-exponential phase (OD_{600} ~ 0.2) in GM17 medium at 37°C (with 0.15 mM $ZnSO_4$ where relevant) and 84 ml of culture was mixed by inverting with 8.4 ml of fixing solution [50 mM Tris pH 8.0, 100 mM NaCl, 0.5 mM EGTA, 1 mM EDTA, 30% (v/v) formaldehyde] and incubated at room temperature for 30 min. Cells were washed and sonicated as described in the supplementary information. Immunoprecipitation was performed using anti-GFP antibodies (rabbit serum, polyclonal, Invitrogen A-6455) and proteinG coupled Dyna Beads (Invitrogen) as described in more detail in the supplementary information.

Real-time qPCR

Real-time qPCR was performed using MESA Fast qPCR Master Mix from Eurogentec in a 72-well rotor in a QIAGEN Roto-Gene Q according to Manufacturer's instructions. CT values were calculated using the Real-time PCR miner software (http://www.miner.ewindup.info/) (Zhao and Fernald, 2005). Primers used for real-time qPCR are listed in Table S1.

ChIP-on-chip

Input and ChIP DNA (10 ng) from strain MT2 (ParB–GFP) was randomly amplified using the WGA2 kit from Sigma according to the manufacturer's instructions. Next, amplified DNA was fluorescently labelled using the Bioprime Total genomic labelling kit from Invitrogen. Eluate DNA was labelled with AlexA Fluor 3 and input DNA with Alexa Fluor 5 and labelled DNA was hybridized to a DNA-microarray containing amplicons of all open reading frames of *S. pneumoniae* D39 (Kloosterman *et al.*, 2006). The ChIP-on-chip data was deposited at GEO (accession number GSE26839).

Acknowledgements

We thank Anne de Jong for bioinformatics support. We extend special thanks to Jean-Pierre Claverys for excellent comments on the manuscript. L.A. was supported by a postdoctoral fellowship from the European Molecular Biology Organization (EMBO). Work in the lab of S.G. is supported by an ERC-Starting Grant (260853). Work in the lab of J.W.V. is supported by an EU Marie-Curie Reintegration Fellowship, a Sysmo2 Grant (NWO-ALW/ERASysBio), a Horizon grant (ZonMW) and by a VENI fellowship (NWO-ALW).

References

Avery, A.T., MacLeod, C.M., and McCarty, M. (1944) Studies on the chemical nature of the substance inducing transformation of pneumococcal types. Induction of transformation by a desoxyribonucleic acid fraction isolated from *Pneumococcus* type III. *J Exp Med* **79:** 137–158.

Baerends, R.J., Smits, W.K., de Jong, A., Hamoen, L.W., Kok, J., and Kuipers, O.P. (2004) Genome2D: a visualization tool for the rapid analysis of bacterial transcriptome data. *Genome Biol* **5:** R37.

Bloom, K., and Joglekar, A. (2010) Towards building a chromosome segregation machine. *Nature* **463:** 446–456.

Bouthier de la Tour, C., Toueille, M., Jolivet, E., Nguyen, H.H., Servant, P., Vannier, F., and Sommer, S. (2009) The *Deinococcus radiodurans* SMC protein is dispensable for cell viability yet plays a role in DNA folding. *Extremophiles* **13:** 827–837.

Britton, R.A., Lin, D.C., and Grossman, A.D. (1998) Characterization of a prokaryotic SMC protein involved in chromosome partitioning. *Genes Dev* **12:** 1254–1259.

Dagkessamanskaia, A., Moscoso, M., Henard, V., Guiral, S., Overweg, K., Reuter, M., *et al*. (2004) Interconnection of competence, stress and CiaR regulons in *Streptococcus pneumoniae*: competence triggers stationary phase autolysis of *ciaR* mutant cells. *Mol Microbiol* **51:** 1071–1086.

Danilova, O., Reyes-Lamothe, R., Pinskaya, M., Sherratt, D., and Possoz, C. (2007) MukB colocalizes with the *oriC* region and is required for organization of the two *Escherichia coli* chromosome arms into separate cell halves. *Mol Microbiol* **65:** 1485–1492.

Eberhardt, A., Wu, L.J., Errington, J., Vollmer, W., and Veening, J.W. (2009) Cellular localization of choline-utilization proteins in *Streptococcus pneumoniae* using novel fluorescent reporter systems. *Mol Microbiol* **74:** 395–408.

Errington, J. (2010) From spores to antibiotics via the cell cycle. *Microbiology* **156:** 1–13.

Fadda, D., Santona, A., D'Ulisse, V., Ghelardini, P., Ennas, M.G., Whalen, M.B., and Massidda, O. (2007) *Streptococcus pneumoniae* DivIVA: localization and interactions in a MinCD-free context. *J Bacteriol* **189:** 1288–1298.

Ferrandiz, M.J., Martin-Galiano, A.J., Schvartzman, J.B., and de la Campa, A.G. (2010) The genome of *Streptococcus pneumoniae* is organized in topology-reacting gene clusters. *Nucleic Acids Res* **38:** 3570–3581.

Fogel, M.A., and Waldor, M.K. (2006) A dynamic, mitotic-like mechanism for bacterial chromosome segregation. *Genes Dev* **20:** 3269–3282.

Gasc, A.M., Giammarinaro, P., Ton-Hoang, B., Geslin, P., van der Giezen, M., and Sicard, M. (1997) Structural organization of the *Streptococcus pneumoniae* chromosome and relatedness of penicillin-sensitive and -resistant strains in type 9V. *Microb Drug Resist* **3:** 65–72.

Gerdes, K., Howard, M., and Szardenings, F. (2010) Pushing and pulling in prokaryotic DNA segregation. *Cell* **141:** 927–942.

Glaser, P., Sharpe, M.E., Raether, B., Perego, M., Ohlsen, K., and Errington, J. (1997) Dynamic, mitotic-like behavior of a bacterial protein required for accurate chromosome partitioning. *Genes Dev* **11:** 1160–1168.

Graumann, P.L., and Knust, T. (2009) Dynamics of the bacterial SMC complex and SMC-like proteins involved in DNA repair. *Chromosome Res* **17:** 265–275.

Gruber, S., and Errington, J. (2009) Recruitment of condensin to replication origin regions by ParB/SpoOJ promotes chromosome segregation in *B. subtilis*. *Cell* **137:** 685–696.

Guthlein, C., Wanner, R.M., Sander, P., Bottger, E.C., and Springer, B. (2008) A mycobacterial *smc* null mutant is proficient in DNA repair and long-term survival. *J Bacteriol* **190:** 452–456.

Halfmann, A., Kovacs, M., Hakenbeck, R., and Bruckner, R. (2007) Identification of the genes directly controlled by the response regulator CiaR in *Streptococcus pneumoniae*: five out of 15 promoters drive expression of small non-coding RNAs. *Mol Microbiol* **66:** 110–126.

Hendriksen, W.T., Bootsma, H.J., Estevao, S., Hoogenboezem, T., de Jong, A., de Groot, R., *et al*. (2008) CodY of *Streptococcus pneumoniae*: link between nutritional gene regulation and colonization. *J Bacteriol* **190:** 590–601.

Hoskins, J., Alborn, W.E., Jr, Arnold, J., Blaszczak, L.C., Burgett, S., DeHoff, B.S., *et al*. (2001) Genome of the bacterium *Streptococcus pneumoniae* strain R6. *J Bacteriol* **183:** 5709–5717.

Hudson, D.F., Marshall, K.M., and Earnshaw, W.C. (2009) Condensin: architect of mitotic chromosomes. *Chromosome Res* **17:** 131–144.

Hui, M.P., Galkin, V.E., Yu, X., Stasiak, A.Z., Stasiak, A., Waldor, M.K., and Egelman, E.H. (2010) ParA2, a *Vibrio cholerae* chromosome partitioning protein, forms left-handed helical filaments on DNA. *Proc Natl Acad Sci USA* **107:** 4590–4595.

Ireton, K., Gunther, N.W., and Grossman, A.D. (1994) *spo0J* is required for normal chromosome segregation as well as the initiation of sporulation in *Bacillus subtilis*. *J Bacteriol* **176:** 5320–5329.

Jun, S., and Mulder, B. (2006) Entropy-driven spatial organization of highly confined polymers: lessons for the bacterial chromosome. *Proc Natl Acad Sci USA* **103:** 12388–12393.

Jun, S., and Wright, A. (2010) Entropy as the driver of chromosome segregation. *Nat Rev Microbiol* **8:** 600–607.

Katayama, T., Ozaki, S., Keyamura, K., and Fujimitsu, K. (2010) Regulation of the replication cycle: conserved and

diverse regulatory systems for DnaA and *oriC*. *Nat Rev Microbiol* **8:** 163–170.

Kloosterman, T.G., Hendriksen, W.T., Bijlsma, J.J., Bootsma, H.J., van Hijum, S.A., Kok, J., *et al*. (2006) Regulation of glutamine and glutamate metabolism by GlnR and GlnA in *Streptococcus pneumoniae*. *J Biol Chem* **281:** 25097–25109.

Kornberg, A., and Baker, T.A. (1992) *DNA Replication*. New York: W.H. Freeman and Co.

Lanie, J.A., Ng, W.L., Kazmierczak, K.M., Andrzejewski, T.M., Davidsen, T.M., Wayne, K.J., *et al*. (2007) Genome sequence of Avery's virulent serotype 2 strain D39 of *Streptococcus pneumoniae* and comparison with that of unencapsulated laboratory strain R6. *J Bacteriol* **189:** 38–51.

Leenhouts, K., Buist, G., Bolhuis, A., ten Berge, A., Kiel, J., Mierau, I., *et al*. (1996) A general system for generating unlabelled gene replacements in bacterial chromosomes. *Mol Gen Genet* **253:** 217–224.

Lin, D.C., Levin, P.A., and Grossman, A.D. (1997) Bipolar localization of a chromosome partition protein in *Bacillus subtilis*. *Proc Natl Acad Sci USA* **94:** 4721–4726.

Lindow, J.C., Britton, R.A., and Grossman, A.D. (2002) Structural maintenance of chromosomes protein of *Bacillus subtilis* affects supercoiling *in vivo*. *J Bacteriol* **184:** 5317–5322.

Livny, J., Yamaichi, Y., and Waldor, M.K. (2007) Distribution of centromere-like *parS* sites in bacteria: insights from comparative genomics. *J Bacteriol* **189:** 8693–8703.

Lynch, J.P., 3rd, and Zhanel, G.G. (2010) *Streptococcus pneumoniae*: epidemiology and risk factors, evolution of antimicrobial resistance, and impact of vaccines. *Curr Opin Pulm Med* **16:** 217–225.

Martin, B., Garcia, P., Castanie, M.P., and Claverys, J.P. (1995) The *recA* gene of *Streptococcus pneumoniae* is part of a competence-induced operon and controls lysogenic induction. *Mol Microbiol* **15:** 367–379.

Mascarenhas, J., Soppa, J., Strunnikov, A.V., and Graumann, P.L. (2002) Cell cycle-dependent localization of two novel prokaryotic chromosome segregation and condensation proteins in *Bacillus subtilis* that interact with SMC protein. *EMBO J* **21:** 3108–3118.

Mitchell, A.M., and Mitchell, T.J. (2010) *Streptococcus pneumoniae*: virulence factors and variation. *Clin Microbiol Infect* **16:** 411–418.

Moriya, S., Tsujikawa, E., Hassan, A.K., Asai, K., Kodama, T., and Ogasawara, N. (1998) A *Bacillus subtilis* gene-encoding protein homologous to eukaryotic SMC motor protein is necessary for chromosome partition. *Mol Microbiol* **29:** 179–187.

Mott, M.L., and Berger, J.M. (2007) DNA replication initiation: mechanisms and regulation in bacteria. *Nat Rev Microbiol* **5:** 343–354.

Murray, H., and Errington, J. (2008) Dynamic control of the DNA replication initiation protein DnaA by Soj/ParA. *Cell* **135:** 74–84.

Nasmyth, K., and Haering, C.H. (2009) Cohesin: its roles and mechanisms. *Annu Rev Genet* **43:** 525–558.

O'Brien, K.L., Wolfson, L.J., Watt, J.P., Henkle, E., Deloria-Knoll, M., McCall, N., *et al*. (2009) Burden of disease caused by *Streptococcus pneumoniae* in children younger than 5 years: global estimates. *Lancet* **374:** 893–902.

Onn, I., Heidinger-Pauli, J.M., Guacci, V., Unal, E., and Koshland, D.E. (2008) Sister chromatid cohesion: a simple concept with a complex reality. *Annu Rev Cell Dev Biol* **24:** 105–129.

van der Poll, T., and Opal, S.M. (2009) Pathogenesis, treatment, and prevention of pneumococcal pneumonia. *Lancet* **374:** 1543–1556.

Ptacin, J.L., Lee, S.F., Garner, E.C., Toro, E., Eckart, M., Comolli, L.R., *et al*. (2010) A spindle-like apparatus guides bacterial chromosome segregation. *Nat Cell Biol* **12:** 791–798.

Reyes-Lamothe, R., Wang, X., and Sherratt, D. (2008) *Escherichia coli* and its chromosome. *Trends Microbiol* **16:** 238–245.

Ringgaard, S., van Zon, J., Howard, M., and Gerdes, K. (2009) Movement and equipositioning of plasmids by ParA filament disassembly. *Proc Natl Acad Sci USA* **106:** 19369–19374.

Salje, J. (2010) Plasmid segregation: how to survive as an extra piece of DNA. *Crit Rev Biochem Mol Biol* **45:** 296–317.

Sambrook, J. (2001) *Molecular Cloning: A Laboratory Manual*. Cold Spring Harbor, NY: Cold Spring Harbor Laboratory Press.

Schofield, W.B., Lim, H.C., and Jacobs-Wagner, C. (2010) Cell cycle coordination and regulation of bacterial chromosome segregation dynamics by polarly localized proteins. *EMBO J* **29:** 3068–3081.

Scholefield, G., Veening, J.W., and Murray, H. (2011) DnaA and ORC: more than DNA replication initiators. *Trends Cell Biol* **21:** 188–194.

Sebert, M.E., Palmer, L.M., Rosenberg, M., and Weiser, J.N. (2002) Microarray-based identification of *htrA*, a *Streptococcus pneumoniae* gene that is regulated by the CiaRH two-component system and contributes to nasopharyngeal colonization. *Infect Immun* **70:** 4059–4067.

Soppa, J., Kobayashi, K., Noirot-Gros, M.F., Oesterhelt, D., Ehrlich, S.D., Dervyn, E., *et al*. (2002) Discovery of two novel families of proteins that are proposed to interact with prokaryotic SMC proteins, and characterization of the *Bacillus subtilis* family members ScpA and ScpB. *Mol Microbiol* **45:** 59–71.

Sullivan, N.L., Marquis, K.A., and Rudner, D.Z. (2009) Recruitment of SMC by ParB–*parS* organizes the origin region and promotes efficient chromosome segregation. *Cell* **137:** 697–707.

Terzaghi, B.E., and Sandine, W.E. (1975) Improved medium for lactic streptococci and their bacteriophages. *Appl Microbiol* **29:** 807–813.

Thanbichler, M. (2009) Closing the ring: a new twist to bacterial chromosome condensation. *Cell* **137:** 598–600.

Toro, E., and Shapiro, L. (2010) Bacterial chromosome organization and segregation. *Cold Spring Harb Perspect Biol* **2:** a000349.

Weiser, J.N. (2010) The pneumococcus: why a commensal misbehaves. *J Mol Med* **88:** 97–102.

Yu, W., Herbert, S., Graumann, P.L., and Gotz, F. (2010) Contribution of SMC (structural maintenance of chromo-

somes) and SpoIIIE to chromosome segregation in Staphylococci. *J Bacteriol* **192:** 4067–4073.
Zakrzewska-Czerwinska, J., Jakimowicz, D., Zawilak-Pawlik, A., and Messer, W. (2007) Regulation of the initiation of chromosomal replication in bacteria. *FEMS Microbiol Rev* **31:** 378–387.
Zhao, S., and Fernald, R.D. (2005) Comprehensive algorithm for quantitative real-time polymerase chain reaction. *J Comput Biol* **12:** 1047–1064.

Supporting information

Additional supporting information may be found in the online version of this article.

Please note: Wiley-Blackwell are not responsible for the content or functionality of any supporting materials supplied by the authors. Any queries (other than missing material) should be directed to the corresponding author for the article.